

# Journal of Visualized Experiments

## Multimodal Three-dimensional Printing of Phantoms to Simulate Biologic Tissue --Manuscript Draft--

Article Type:	Methods Article - Author Produced Video
Manuscript Number:	JoVE60563R2
Full Title:	Multimodal Three-dimensional Printing of Phantoms to Simulate Biologic Tissue
Section/Category:	JoVE Engineering
Keywords:	three-dimensional printing, optical phantom, spin-coating, polyjet printing, fused deposition modeling
Corresponding Author:	Ronald Xu UNITED STATES
Corresponding Author's Institution:	
Corresponding Author E-Mail:	xu.202@osu.edu
Order of Authors:	Canzhen Ma Shuwei Shen Guangli Liu Siyue Guo Buyun Guo Jialuo Li Kuiming Huang Yidan Zheng Pengfei Shao Erbao Dong Jiaru Chu Ronald X. Xu
Additional Information:	
Question	Response
Please indicate whether this article will be Standard Access or Open Access.	Standard Access (US\$1200)

**TITLE:****Multimodal 3D Printing of Phantoms to Simulate Biologic Tissue****AUTHORS AND AFFILIATIONS:**

Canzhen Ma<sup>1,2\*</sup>, Shuwei Shen<sup>1,2\*</sup>, Guangli Liu<sup>1</sup>, Siyue Guo<sup>1,2</sup>, Buyun Guo<sup>1,2</sup>, Jialuo Li<sup>1,2</sup>, Kuiming Huang<sup>1,2</sup>, Yidan Zheng<sup>1</sup>, Pengfei Shao<sup>1,2</sup>, Erbao Dong<sup>1,2</sup>, Jiaru Chu<sup>1</sup>, Ronald X. Xu<sup>1,2,3</sup>

<sup>1</sup>Department of Precision Machinery and Precision Instrumentation, University of Science and Technology of China, Hefei, Anhui, China

<sup>2</sup>Key Laboratory of Precision Scientific Instrumentation of Anhui Higher Education Institutes, University of Science and Technology of China, China

<sup>3</sup>Department of Biomedical Engineering, The Ohio State University, Columbus, OH, USA

\*These authors contributed equally.

**Corresponding Author:**

Ronald X. Xu (xu.ronald@hotmail.com)

**Email Addresses of Co-Authors:**

Canzhen Ma (mcanzhen@mail.ustc.edu.cn)

Shuwei Shen (swshen@mail.ustc.edu.cn)

Guangli Liu (Liugl@mail.ustc.edu.cn)

Siyue Guo (siyue@mail.ustc.edu.cn)

Buyun Guo (tcbuyun@mail.ustc.edu.cn)

Jialuo Li (zkd@mail.ustc.edu.cn)

Kuiming Huang (hkm1995@mail.ustc.edu.cn)

Yidan Zheng (zhengyid@mail.ustc.edu.cn)

Pengfei Shao (spf@ustc.edu.cn)

Erbao Dong (ebdong@ustc.edu.cn)

Jiaru Chu (jrchu@ustc.edu.cn)

**KEYWORDS:**

three-dimensional printing, optical phantom, spin coating, polyjet printing, fused deposition modeling, multimodal characterization

**SUMMARY:**

Spin coating, polyjet printing, and fused deposition modeling are integrated to produce multilayered heterogeneous phantoms that simulate structural and functional properties of biological tissue.

**ABSTRACT:**

Biomedical optical imaging is playing an important role in diagnosis and treatment of various diseases. However, the accuracy and the reproducibility of an optical imaging device are greatly affected by the performance characteristics of its components, the test environment, and the

operations. Therefore, it is necessary to calibrate these devices by traceable phantom standards. However, most of the currently available phantoms are homogeneous phantoms that cannot simulate multimodal and dynamic characteristics of biological tissue. Here, we show the fabrication of heterogeneous tissue-simulating phantoms using a production line integrating a spin coating module, a polyjet module, a fused deposition modeling (FDM) module, and an automatic control framework. The structural information and the optical parameters of a "digital optical phantom" are defined in a prototype file, imported to the production line, and fabricated layer-by-layer with sequential switch between different printing modalities. Technical capability of such a production line is exemplified by the automatic printing of skin-simulating phantoms that comprise the epidermis, dermis, subcutaneous tissue, and an embedded tumor.

## INTRODUCTION:

Biomedical optical imaging represents a family of medical imaging tools that detect diseases and tissue anomalies based on light interactions with biological tissue. In comparison with other imaging modalities, such as magnetic resonance imaging (MRI) and computed tomography (CT), biomedical optical imaging takes the advantage of noninvasive measurement of tissue structural, functional, and molecular characteristics using low-cost and portable devices<sup>1-4</sup>. However, despite its superiority in cost and portability, optical imaging has not been widely accepted for clinical diagnosis and therapeutic guidance, partially due to its poor reproducibility and lack of quantitative mapping between optical and biological parameters. The main reason for this limitation is the lack of traceable standards for quantitative calibration and validation of biomedical optical imaging devices.

In the past, a variety of tissue-simulating phantoms were developed for biomedical optical imaging research in various tissue types, such as brain<sup>5-7</sup>, skin<sup>8-12</sup>, bladder<sup>13</sup>, and breast tissues<sup>14-17</sup>. These phantoms are primarily produced by one of the following fabrication processes: 1) spin coating<sup>10,18</sup> (for simulating homogenous and thin-layered tissue); 2) molding<sup>19</sup> (for simulating bulky tissue with geometric features); and 3) three-dimensional (3D) printing<sup>20-22</sup> (for simulating multilayered heterogeneous tissue). Skin phantoms produced by molding are able to mimic the bulk optical properties of skin tissue but cannot simulate the lateral optical heterogeneities<sup>19</sup>. Bentz et al. used a two-channel FDM 3D printing method to mimic different optical properties of biological tissue<sup>23</sup>. However, using two materials cannot sufficiently simulate tissue optical heterogeneity and anisotropy. Lurie et al. created a bladder phantom for optical coherence tomography (OCT) and cystoscopy by combining 3D printing and spin coating<sup>13</sup>. However, heterogeneous features of the phantom, such as blood vessels, had to be hand painted.

Among the above phantom fabrication processes, 3D printing provides the most flexibility for simulating the structural and functional heterogeneities of biological tissue. However, many biological tissue types, such as skin tissue, consist of multilayered and multiscaled components that cannot be effectively duplicated by a single 3D printing process. Therefore, integration of multiple manufacturing processes is necessary. We propose a 3D printing production line that integrates multiple manufacturing processes for automatic production of multilayered and multiscaled tissue simulating phantoms as a traceable standard for biomedical optical imaging (**Figure 1**). Although spin coating, polyjet printing, and FDM are automated in our 3D printing

production line, each modality retains the same functional characteristics as the established processes. Therefore, this paper provides a general guideline for producing multiscaled, multilayered, and heterogeneous tissue-simulation phantoms without the need for physical integration of multiple processes in a single apparatus.

[Place **Figure 1** here]

## **PROTOCOL:**

### **1. Preparing materials for 3D printing**

NOTE: Our optical phantom production line uses a variety of printing materials to simulate the structural and functional heterogeneities of biological tissue. The selection of the printing materials also depends on the manufacturing processes.

#### **1.1. Material preparation for spin coating printing**

1.1.1. Add 100 mg of titanium dioxide (TiO<sub>2</sub>) powder into a beaker containing 100 mL of stereolithography (SLA) photopolymer resin.

1.1.2. Stir the mixture in the beaker for 30 min on a magnetic stirrer.

1.1.3. Seal the beaker with tinfoil and sonicate it in an ultrasonic machine for 15 min.

1.1.4. Vacuum the material for 10 min and load it into the storage syringe of the device.

#### **1.2. Material preparation for polyjet printing**

1.2.1. Add 17.56 g of 2-hydroxy-2-methylpropiophenone (1-hydroxycyclohexyl phenyl ketone) into the beaker containing 80 g of triethylene glycol dimethacrylate to get 18% (w/w) material.

1.2.2. Seal the beaker with tinfoil and sonicate it in an ultrasonic machine for 15 min.

1.2.3. Take out 20 mL of the mixture and add 5 mg of the oil-soluble Chinese red dye into it. Repeat step 1.2.2.

1.2.4. Vacuum all the materials, load the solution with dye into the cartridges for the Y (Yellow) channel, and load the pure solution into the cartridges for the K (Black) channel.

#### **1.3. Material preparation for FDM printing**

1.3.1. Load 200 g of gel wax into each of three beakers and then heat them to 60 °C on a magnetic stirrer.

1.3.2. Add 600 mg  $\text{TiO}_2$  powder into the first beaker. Add 80 mg of graphite powder into the second one.

1.3.3. Stir the gel wax mixed with  $\text{TiO}_2$  and gel wax mixed with graphite powder in different beakers for 30 min on the magnetic stirrer.

1.3.4. Vacuum the three different materials for 2 min and load them into the extruder of the hybrid-three-nozzle module before solidification.

## **2. Preparing computer models for multimodal 3D printing**

NOTE: The heterogeneous skin tissue is simplified into three layers: the epidermis, dermis, and subcutaneous tissue layer. The epidermis layer is produced by spin coating using the material introduced in step 1.1. The dermis layer is produced by polyjet printing using the photosensitive polymer introduced in step 1.2. The subcutaneous tissue layer is produced by FDM using the material introduced in step 1.3. A prototype computer aided design (CAD) file of different printing parameters is designed to implement the aforementioned fabrication processes.

### **2.1. Design of a digital optical phantom for skin**

2.1.1. Design the skin phantom with the following three layers: an epidermis layer 100  $\mu\text{m}$  thick, a dermis layer 400  $\mu\text{m}$  thick, and a subcutaneous tissue 1 cm thick.

2.1.2. Draw a tumor model using a 3D modeling software package (e.g., Solidworks) (**Figure 5A**).

### **2.2. Parameter setting for spin coating**

2.2.1. Set the parameters of rotating speed and duration in the control software of the printing device. The first-stage spin coating speed used in this demonstration is 200 revolutions per min (rpm), the spin coating time is 20 s, the speed in the second-stage spin coating is 1,000 rpm, and the spin coating time is 40 s.

2.2.2. Set the amount of spin coating material as 3 mL and the time of light-curing as 180 s in the control software.

### **2.3. Preparation of the source file for polyjet printing**

2.3.1. Import the blood vessel image to be printed into the AcroRIP Color software package and set the parameters (printing position and inkjet amount) according to the relationship between the optical parameters of the printed phantoms and the image properties. In this printed blood vessel picture, the K channel is loaded with a transparent photocurable material, and the Y channel is loaded with a photocurable material with Chinese red dye.

2.3.2. Generate a “.prn” file with parameters defined for 3D printing.

## 2.4. Preparation of G code for FDM printing

2.4.1. Draw a frustum model with a 3D mapping software package (e.g., Solidworks) to simulate a tumor.

2.4.2. Import the “.stl” file of the tumor model into a Cura software package installed with an all-in-one nozzle slicing script.

2.4.3. Slice the model to generate the G code required for printing.

## 2.5. Loading of the documents to the printing control software

2.5.1. Click the "File" menu item in the menu bar, select the "Import UV Print File" submenu item, and load the UV printing “.prn” files introduced in step 2.3.

2.5.2. Load the G code generated in step 2.4 into the print control software as in step 2.5.1.

2.5.3. Click the **Start Printing** button to start the automated 3D print procedure.

## 3. Printing the skin epidermis layer phantom component by spin coating

NOTE: The spin coating module is mainly comprised of three parts: 1) a spin coater; 2) a glue dispenser; and 3) a UV lamp.

3.1. Move the substrate on the loading station to the sample stage of the spin coater with a mechanical hand. Start the vacuum pump to fix the substrate by adsorption.

3.2. The glue dispenser controls the syringe to drip the material introduced in step 2.2.2 at the center of the substrate.

3.3. The spin coater starts to work following the set speed and time parameters.

3.4. Put down the UV lamp (wavelength = 395 nm) and turn the it on for 180 s.

3.5. Lift the UV lamp, turn off the spin-coater, and the skin epidermis is printed.

## 4. Printing the skin dermis layer phantom component by polyjetting

NOTE: The polyjet printing module consists of a piezoelectric inkjet nozzle, a three-dimensional mobile platform, a control panel, and a UV lamp (mercury lamp). The solvent-based photocurable material, absorption material, and scattering material are used as a matrix. Different optical parameters are obtained by spraying materials in different proportions in different regions. Finally, the dermis layer phantom is printed and cured layer-by-layer.

4.1. Move the substrate to the 3D mobile platform and open the suction valve to adsorb the substrate on the platform.

4.2. The 3D mobile platform holds the substrate to the initial position of the UV print.

4.3. Push the inkjet printer to the working position by the cylinder, and the inkjet printer works the time specified in the “.prn” file sent by the host computer. Here, the paper feed signal of the inkjet printer is used to drive the movement of the Y-axis mobile platform.

4.4. The inkjet printer prints the layer designed in step 2.5.1 and the cylinder pushes the inkjet printer back to the original position. The Y-axis of the 3D moving platform placed with the substrate is initialized by moving to its initial position.

4.5. The substrate moves 50 mm in the positive direction of the Y-axis. The UV lamp is pushed down by the cylinder (10 mm above the substrate).

4.6. Turn on the UV lamp for 180 s according to the curing time setting.

4.7. Push the UV lamp to the initial position with the cylinder. The Y-axis of the 3D mobile platform placed with the substrate is initialized and returned to its initial position.

4.8. Move the 3D mobile platform placed with substrate down by 0.1 mm along the Z-axis.

4.9. Repeat steps 4.1–4.8 to print the next layer until the multilayer printing is completed.

## **5. Printing the subcutaneous tissue phantom component by FDM**

NOTE: The FDM module is comprised of a hybrid-three-head module, a single-head module, and a 3D mobile platform. The gel wax, the absorbing material, and the scattering material are used as raw materials to prepare a phantom simulating subcutaneous tissue/tumor. The gel wax is heated and melted in the feeder. Uniformly stirred by the extrusion head, it is extruded to print the final phantoms with the desired optical parameters.

5.1. Turn on the heating power of the nozzle module and set the temperature to 60 °C.

5.2. Move the mixing nozzle to the working position by pushing the cylinder.

5.3. The FDM module receives the G code commands sent by the host computer, and the mixing nozzle is heated up to 68 °C.

5.4. Turn on the agitation motor and mix the materials well.

5.5. Initialize the 3D mobile platform and the XYZ axes will move to the initial position.

5.6. The printing process is executed following the G code commands. In a layer-by-layer printing procedure, the materials are extruded in proportion to the mixing ratio that determine the optical parameters of the phantom in each layer. The printing is complete when the subcutaneous tissue portion or the tumor portion is fully printed.

5.7. Move the mixing nozzle module to the initial position by pushing the cylinder.

CAUTION: Because graphite powder has strong light absorption, it needs to be mixed as uniformly as possible to avoid changes in the optical parameters induced by aggregation.  $\text{TiO}_2$  powder of large particle size easily precipitates and affects material placement accuracy, so it is necessary to fully mix it.  $\text{TiO}_2$  should be replaced if stored for a long time.

## **6. Moving the substrate back to the loading station**

6.1. Initialize the 3D mobile platform and move the XYZ axis to the initial position. Move the 3D mobile platform to the handover location.

6.2. Move the mechanical hand to the position above the substrate by pushing the cylinder.

6.3. Pick up the substrate and move it over the loading station with the mechanical hand. Place the substrate on the loading station and complete the automated printing.

## **7. Casting the subcutaneous tissue layer phantom component by molding**

NOTE: If the tumor model for the phantom is designed, it will be necessary to cast the entire phantom by pouring the polydimethylsiloxane (PDMS) outside the tumor. Steps 7.1–7.3 are not required for the FDM module to print subcutaneous tissue layer without a tumor.

7.1. Press on a substrate with a rectangular mold.

7.2. Pour liquid PDMS into the mold.

7.3. Place the substrate in an incubator and store at 60 °C for 2 h.

7.4. Remove the phantom from the substrate.

## **REPRESENTATIVE RESULTS:**

### **Phantom fabricated by spin coating**

The spin coating evenly distributes the droplets on the substrate by rotating the turntable, and a single layer of the original body is fabricated after curing. The rotational speed of the substrate and the time of rotation not only affect the surface quality of the phantom, but also determine the thickness of each layer of the phantom. Phantoms of different thicknesses can be fabricated by repetitive spin coating layer-by-layer. The optical parameters of the phantoms can be



determined by changing the proportion of scattering and absorption materials, as described in our previous publication<sup>24</sup>. Increasing the TiO<sub>2</sub> concentration in the photocurable resin will increase the scattering coefficient of the phantom. Considering that spin coating has a precision of 0.01 mm and the skin epidermis is between 0.04–1.6 mm thick, the process satisfies the requirement for simulating the skin epidermis (**Figure 2**).

[Place **Figure 2** here]

#### **Phantom fabricated by polyjet printing<sup>12</sup>**

Light-curable materials from different channels are mixed with different optical particles and printed by piezoelectric inkjets on a substrate according to the “.prn” file. A single layer of the phantom is obtained after curing. The resolution of the polyjet printer is 18 μm x 18 μm x 10 μm (length x width x height), the positional resolution of the mobile platform is 1 μm, and the nozzle supports four different types of printing materials. The accuracy of the printing plane is 50 μm, and the thickness of each layer is determined by the amount of the ejected materials. As the ejection amount of a single channel is set at 60%, the mean thickness of each layer is 100 ± 10 μm. The dermis layer of skin tissue is typically between 0.4–2.4 mm thick, and the inkjet printing module is able to reach a thickness resolution of 100 μm. The epidermal blood vessels are simulated by mixing the printing materials with Chinese red dye (**Figure 3**).

[Place **Figure 3** here]

#### **Phantom fabricated by FDM printing**

Gel wax is mixed with graphite powder and TiO<sub>2</sub> powder and printed in a desired shape by FDM printing. The dimensional error in the horizontal direction of the phantom is less than 1%. The lateral length of the phantom exceeds 20 mm, the minimally printable feature is 1 mm, and the printable range is 100 mm x 100 mm x 20 mm. The absorption and scattering parameters of a phantom depend on the ratio of the TiO<sub>2</sub> and graphite powder inside. **Figure 4** presents phantoms of different feature sizes printed by the FDM printing using the gel wax without TiO<sub>2</sub> and graphite powder. We can change the ratio of TiO<sub>2</sub> to graphite powder during printing, and thus fabricate phantoms of different absorption and scattering parameters, including gradients (**Figure 4B**). The correlation of absorption and scattering parameters with the ratio of TiO<sub>2</sub> to graphite powder can be found in the references<sup>24</sup>.

[Place **Figure 4** here]

#### **Phantom fabricated by automated printing production line**

By integrating the above three printing methods and following the aforementioned protocol, the production line system is able to produce a tumor-simulating phantom. Taking a simplified skin model as an example, the epidermis layer, the dermis layer, and the subcutaneous tissue layer with different thicknesses and optical properties are fabricated by spin coating, polyjet printing, and FDM printing, respectively. Therefore, the possibility of combining spin coating, polyjet printing, and FDM printing to produce optical phantoms was verified, and the system was able to produce tissue optical phantoms with the simulated optical and structural characteristics

(Figure 5, Figure 6).

[Place Figure 5 here]

[Place Figure 6 here]

#### FIGURE AND TABLE LEGENDS:

**Figure 1: The CAD diagram of the 3D printing production line.** (A) The 3D printing production line with the top shell removed. (B) The schematic of the spin coating module and the mechanical hand module. (C) The schematic of the polyjet printing module. (D) The schematic of the FDM printing module (the UV lamp belongs to the polyjet printing module).

**Figure 2: A single layer phantom fabricated by spin coating.** (A) The PDMS material is added to 50% proportional tert-butyl alcohol and spin-coated at 3,000 rpm for 40 s to form the single layer phantom. The thickness of the phantom is  $10 \pm 1 \mu\text{m}$  as measured by OCT. (B) Correlations between the achievable thickness of the PDMS film and the spin speed at different spinning times.

**Figure 3: Blood vessel simulations printed by polyjet printing.** (A) Blood vessel picture for printing lines mimicking blood vessels. (B) The lines mimicking blood vessels printed on a white paper, where the paper is fixed on the substrate of the 3D mobile platform in the printing process.

**Figure 4: Results of FDM printing.** (A) An eight-layer 40 mm x 40 mm x 0.4 mm cuboid model with gradient color. (B) Gradient phantom obtained by printing the gel wax mixed with  $\text{TiO}_2$  and graphite powder in a gradual scale. (C) CAD model in multi-corner shape. (D) Multi-corner model printed. The bottom right of the picture is the result measured under a front view microscope. The minimum print feature of FDM is 1 mm. (E) Cuboid phantoms printed in the FDM module. (F) The measured results indicate that the variation in size is less than 1% when the lateral dimension is above 20 mm.

**Figure 5: Fabricated multilayer skin phantoms with an embedded tumor.** (A) A schematic diagram of a multilayered structure of a tumor phantom, including one spin-coated layer, seven polyjet printed layers (including three transparent layers and three layers of blood vessel layers, and one common layer, and one FDM printed tumor). The bottom right of the picture is a schematic rendering of the phantom. (B) The phantom on the left has two embedded tumors and the right one has one embedded tumor.

**Figure 6: Fabricating multilayered skin-mimicking phantoms.** (A) A multilayered skin phantom printed on a silicon wafer consists of a spin coating layer, a polyjet printing layer, and an FDM printing layer from bottom to top. (B) Front view of the phantom embedded with blood vessel-like grooves on its surface. (C) Microscopic image of a cross-section of the phantom showing the different layers.

#### DISCUSSION:

In the fabrication of the multilayered phantom, the material used for spin coating is a kind of

light-curable material instead of PDMS. The intermediate layer is printed with the polyjet printing method, which uses the light-curable resin as raw material. Although thin PDMS phantoms can be made by spin coating after adding tert-butyl alcohol, a PDMS layer cannot effectively bind to the light-curable material during polyjet printing. Therefore, we chose the light-curable resin for spin coating.

Currently, only two materials are available for polyjet printing. The addition of TiO<sub>2</sub> powder and Indian ink to the light-curable material simulates the optical properties of the dermis layer, which can be added into the system in future work.

For FDM printing, the materials should be thoroughly mixed before extrusion. Therefore, the process delay due to mixing may be longer than for the traditional FDM printing process. The movement of the substrate on the 3D mobile platform is also delayed for the corresponding time during printing. To print phantoms with complex shapes, control of the delay needs to be improved.

The last step in the fabrication of the tumor-simulating phantom is casting. In fact, in the design of the nozzle assembly, an added nozzle is used to inject a fourth material. However, the control of the movement process of the 3D mobile platform is complicated, and the nozzle may destroy the original tumor model. This can be improved by redesigning the motion control program.

#### **ACKNOWLEDGMENTS:**

The work was supported by the National Natural Science Foundation of China (Grant Nos. 11002139 and 81327803) and the Fundamental Research Funds for the Central Universities. We thank Zachary J. Smith of the University of Science and Technology for providing the audio voiceover.

#### **DISCLOSURES:**

The authors have nothing to disclose.

#### **REFERENCES:**

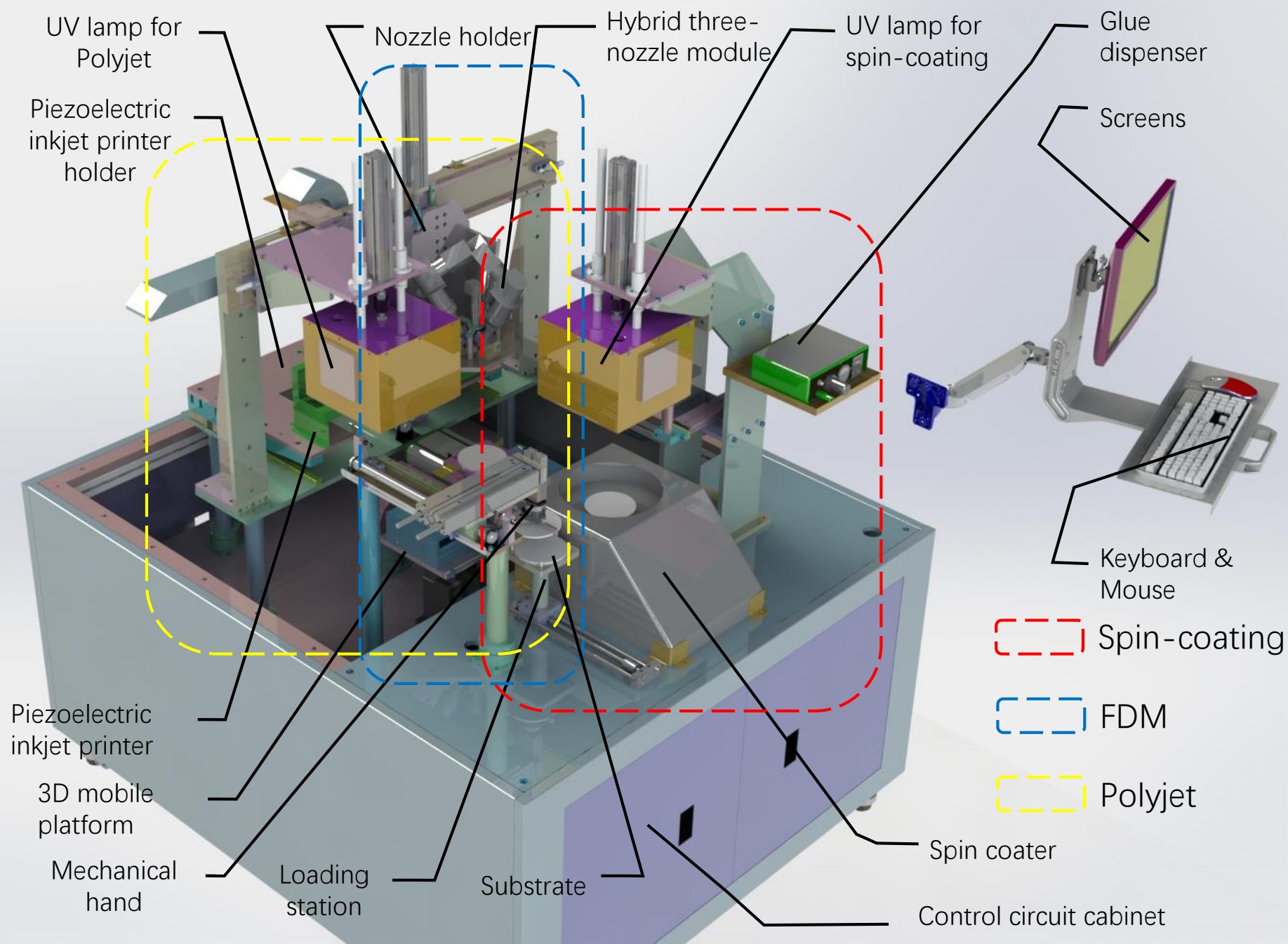
1. Lu, G., Fei, B. Medical hyperspectral imaging: a review. *Journal of Biomedical Optics*. **19** (1), 010901 (2014).
2. Wang, K. et al. Development of a non-uniform discrete Fourier transform based high speed spectral domain optical coherence tomography system. *Optics Express*. **17** (14), 12121–12131 (2009).
3. Zhao, H., Gao, F., Tanikawa, Y., Homma, K., Yamada, Y. Time-resolved diffuse optical tomographic imaging for the provision of both anatomical and functional information about biological tissue. *Applied Optics*. **44** (10), 1905–1916 (2005).
4. Ding, Z., Ren, H., Zhao, Y., Nelson, J. S., Chen, Z. High-resolution optical coherence tomography over a large depth range with an axicon lens. *Optics Letters*. **27** (4), 243–245 (2002).
5. Iida, H. et al. Three-dimensional brain phantom containing bone and grey matter structures with a realistic head contour. *Annals of Nuclear Medicine*. **27** (1), 25–36 (2013).
6. Mobashsher, A. T., Abbosh, A. Three-dimensional human head phantom with realistic

- electrical properties and anatomy. *IEEE Antennas and Wireless Propagation Letters*. **13**, 1401–1404 (2014).
7. Li, J.-B. et al. A new head phantom with realistic shape and spatially varying skull resistivity distribution. *IEEE Transactions on Biomedical Engineering*. **61** (2), 254–263 (2013).
8. Bykov, A. et al. Multilayer tissue phantoms with embedded capillary system for OCT and DOCT imaging. in *Life Sciences*. (International Society for Optics and Photonics) 73760F (2011).
9. Bykov, A. V., Popov, A. P., Priezzhev, A. V., Myllylä, R. Skin phantoms with realistic vessel structure for OCT measurements in Laser Applications. in *European Conference on Biomedical Optics*. (Optical Society of America) 80911R (2010).
10. Park, J. et al. Fabrication of double layer optical tissue phantom by spin coating method: mimicking epidermal and dermal layer. in *Design and Performance Validation of Phantoms Used in Conjunction with Optical Measurement of Tissue V*. (International Society for Optics and Photonics) 85830G (2013)
11. Wróbel, M. S. et al. Use of optical skin phantoms for preclinical evaluation of laser efficiency for skin lesion therapy. *Journal of Biomedical Optics*. **20** (8), 085003 (2015).
12. Sheng, S., Wu, Q., Han, Y., Dong, E., Xu, R. Fabricating optical phantoms to simulate skin tissue properties and microvasculature. in *Design and Performance Validation of Phantoms Used in Conjunction with Optical Measurement of Tissue Vii*. (International Society for Optics and Photonics) 932507 (2015).
13. Lurie, K. L., Smith, G. T., Khan, S. A., Liao, J. C., Ellerbee, A. K. Three-dimensional, distendable bladder phantom for optical coherence tomography and white light cystoscopy. *Journal of Biomedical Optics*. **19** (3), 36009 (2014).
14. Hahn, C., Noghianian, S. Heterogeneous breast phantom development for microwave imaging using regression models. *Journal of Biomedical Imaging*. **2012**, 6 (2012).
15. Ansari, M. A., Mohajerani, E. Estimation of optical abnormalities in breast phantom by diffuse equation. *Optik-International Journal for Light and Electron Optics*. **125** (20), 5978–5981 (2014).
16. Roman, M., Gonzalez, J., Carrasquilla, J., Erickson, S. J., Godavarty, A. A Gen-2 Hand-Held Optical Imager: Phantom and Preliminary in-vivo Breast Imaging Studies. in *29th Southern Biomedical Engineering Conference*. 103–104 (2013).
17. Michaelsen, K. E. et al. Anthropomorphic breast phantoms with physiological water, lipid, and hemoglobin content for near-infrared spectral tomography. *Journal of Biomedical Optics*. **19** (2), 026012 (2014).
18. Park, J. et al. Optical tissue phantoms based on spin coating method. in *Design and Performance Validation of Phantoms Used in Conjunction with Optical Measurement of Tissue VII*. (International Society for Optics and Photonics) 93250A (2015).
19. Mustari, A. et al. Agarose-based tissue mimicking optical phantoms for diffuse reflectance spectroscopy. *Journal of Visualized Experiments*. (138), e57578 (2018).
20. Luciano, N. J. et al. Utilizing 3D printing technology to merge MRI with histology: A protocol for brain sectioning. *Journal of Visualized Experiments*. (118), e54780 (2016).
21. Dong, E. et al. Three-dimensional fuse deposition modeling of tissue-simulating phantom for biomedical optical imaging. *Journal of Biomedical Optics*. **20** (12), 121311 (2015).
22. Beltrame, E. D. V. et al. 3D Printing of Biomolecular Models for Research and Pedagogy. *Journal of Visualized Experiments*. (121), e55427 (2017).

- 485 23. Bentz, B. Z., Chavan, A. V., Lin, D., Tsai, E. H., Webb, K. J. Fabrication and application of  
486 heterogeneous printed mouse phantoms for whole animal optical imaging. *Applied Optics*. **55**  
487 (2), 280–287 (2016).
- 488 24. Liu, G. et al. Fabrication of a multilayer tissue-mimicking phantom with tunable optical  
489 properties to simulate vascular oxygenation and perfusion for optical imaging technology.  
490 *Applied Optics*. **57** (23), 6772–6780 (2018).  
491

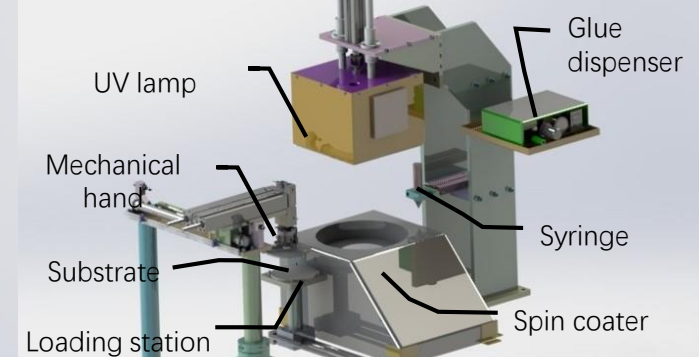
Figure 1

a

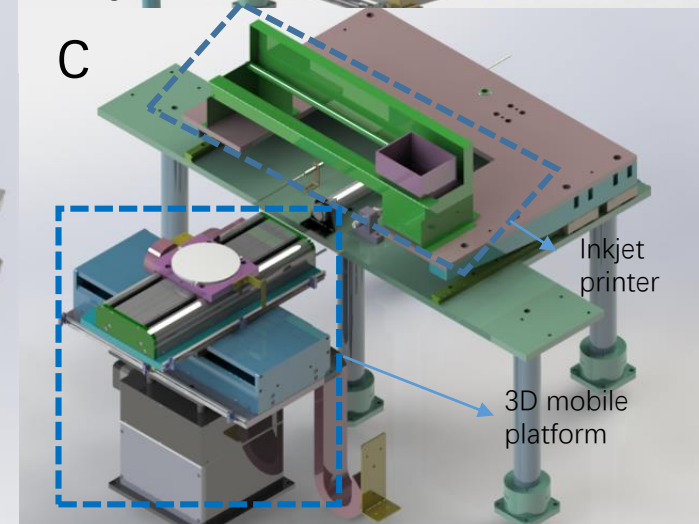


[Click here to access/download;Figure;Figure 1.pdf](#)

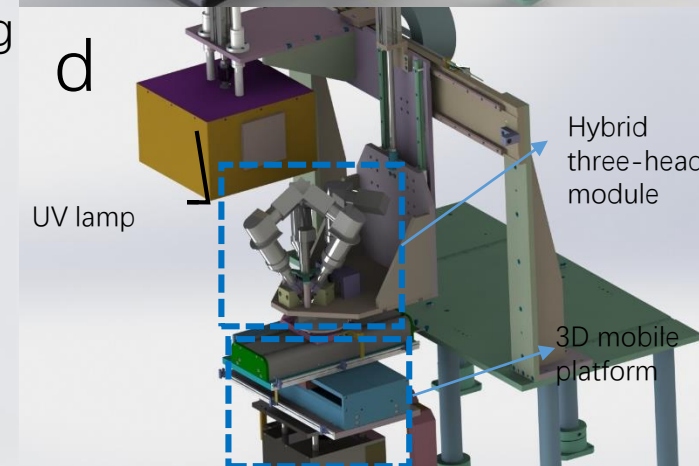
b



c



d

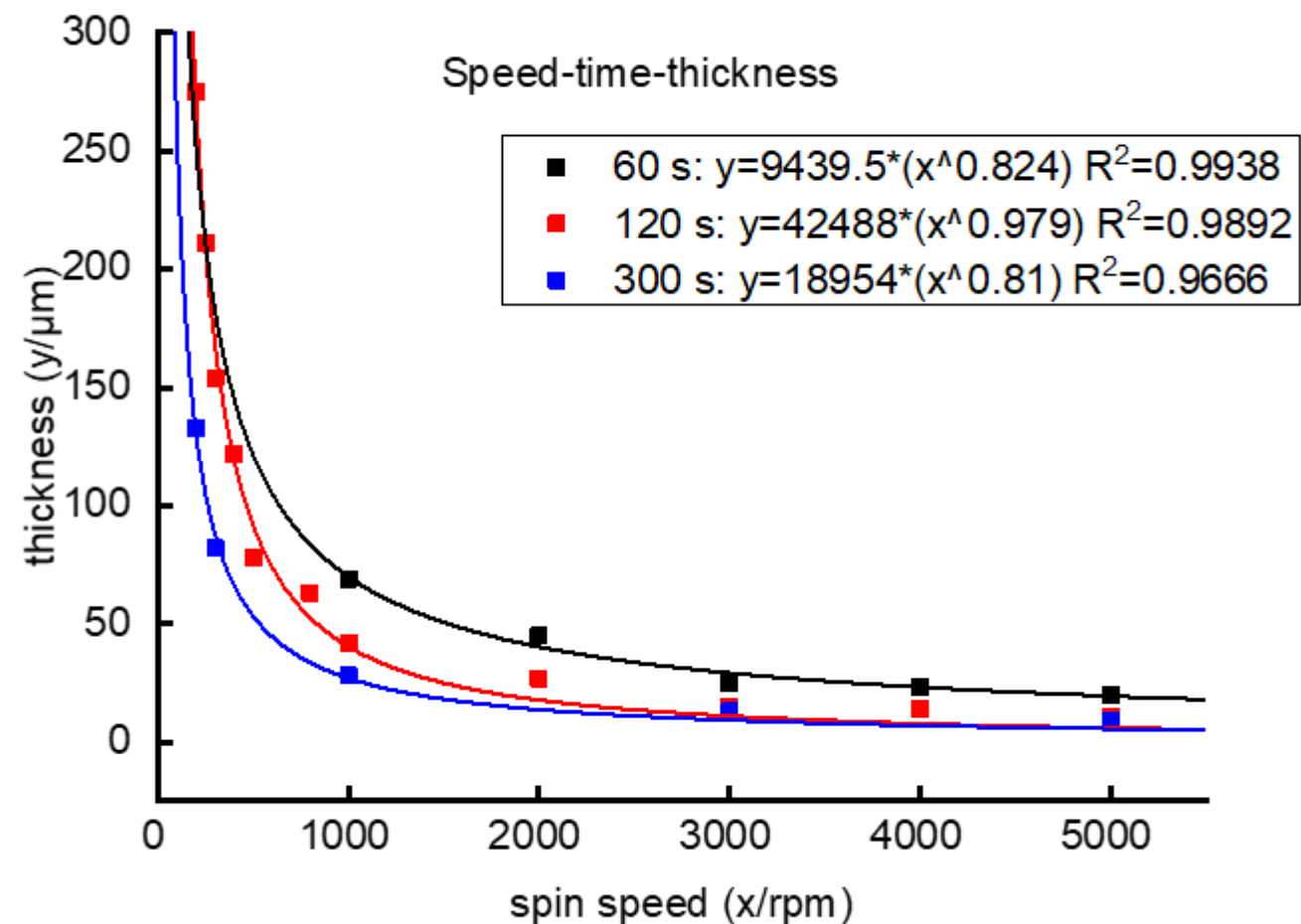


a



100  $\mu\text{m}$

b





a

b

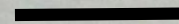
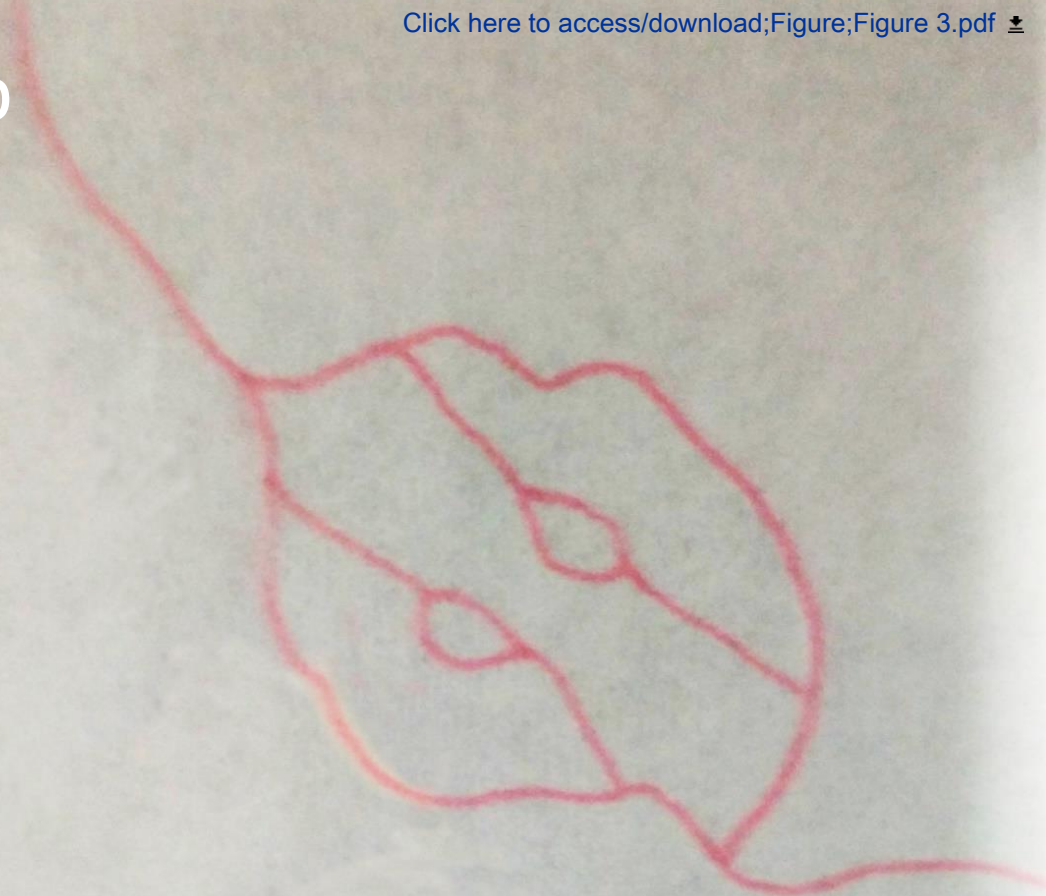
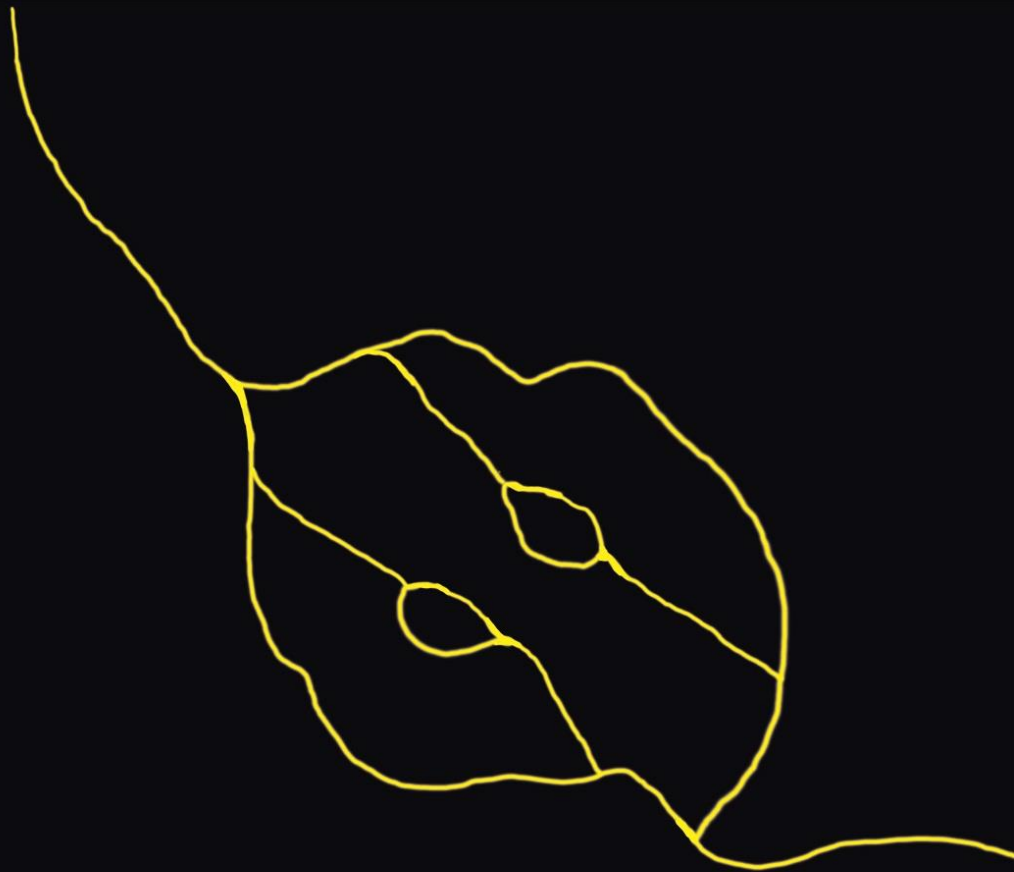
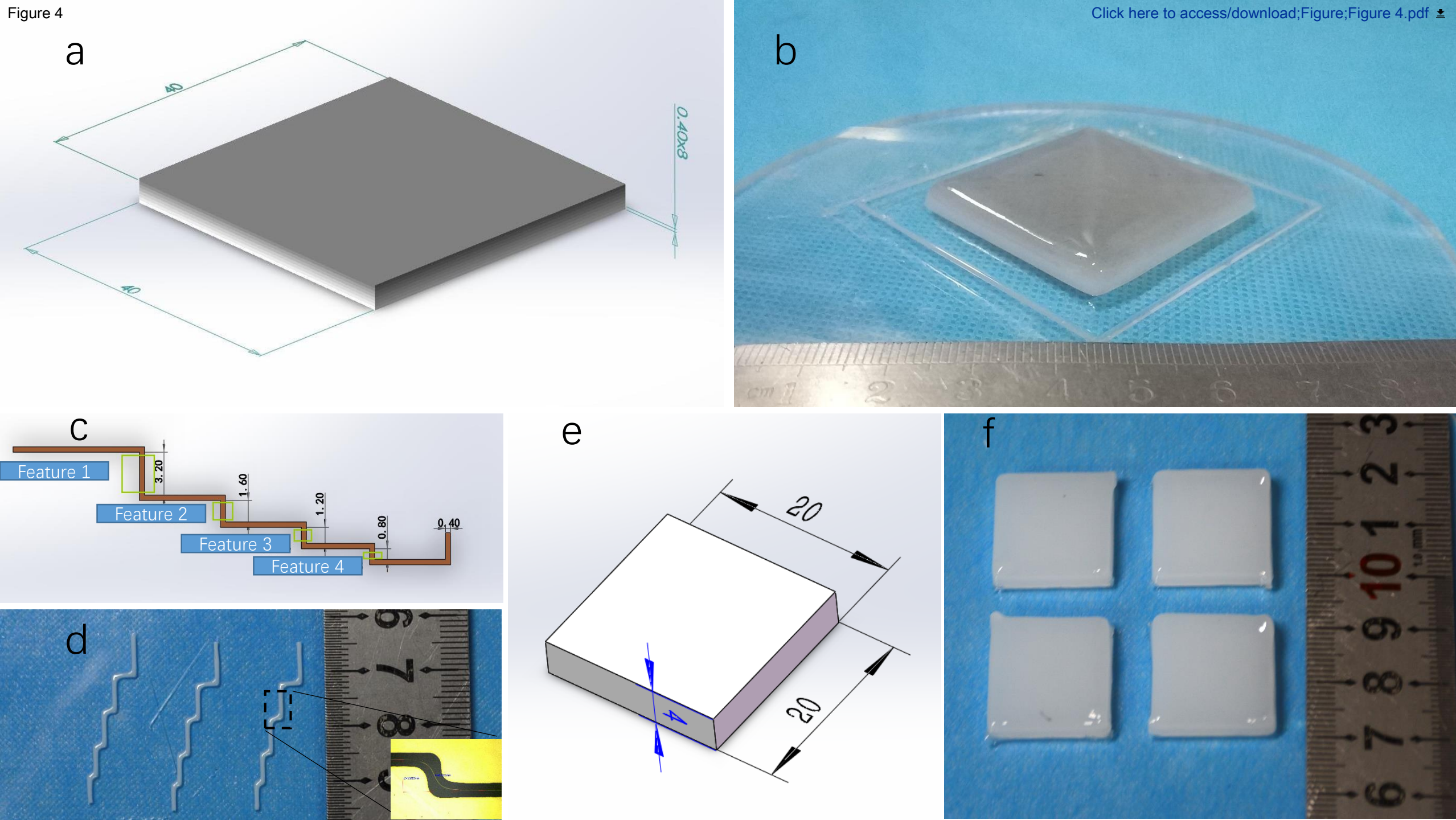
  
10 mm

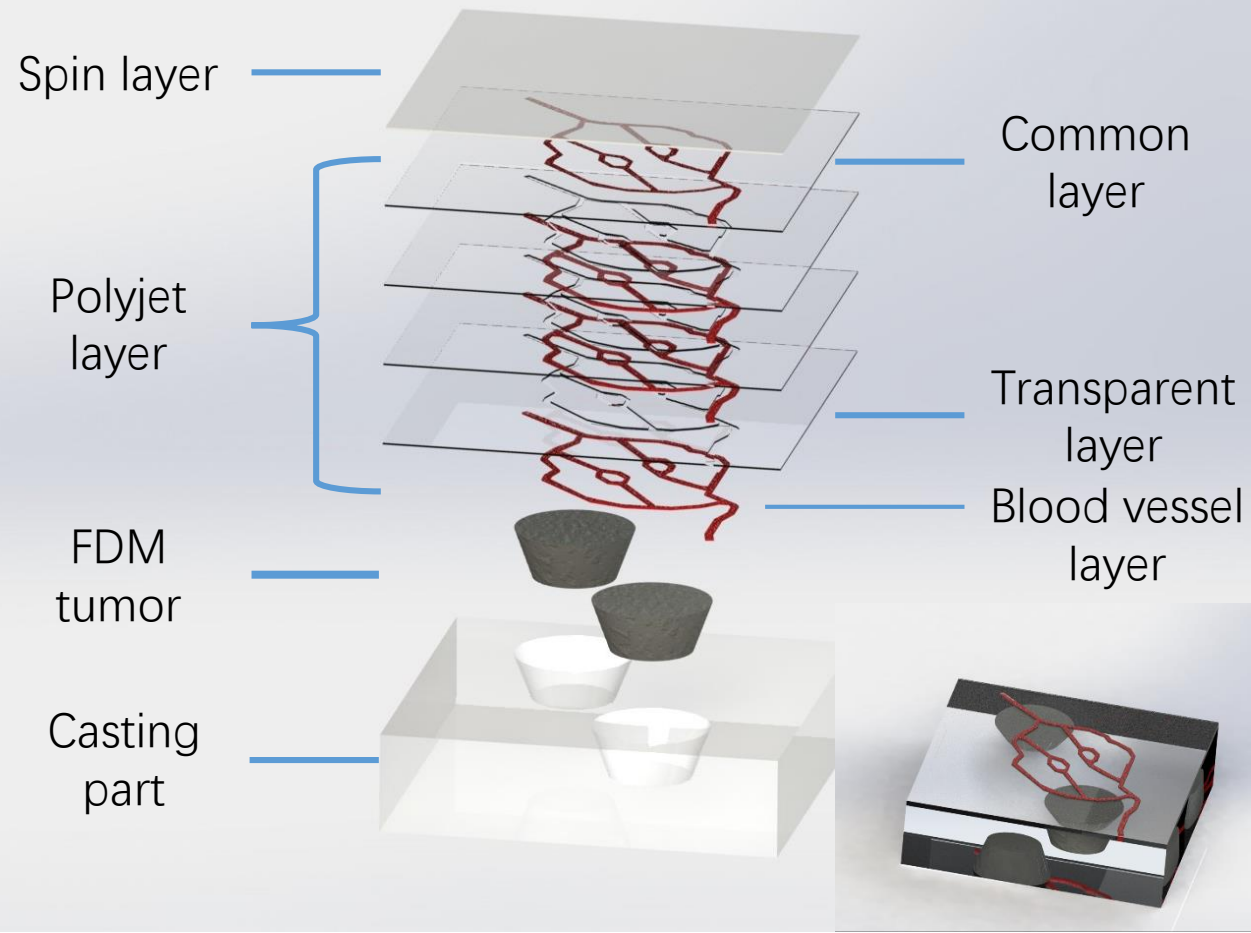


Figure 4

[Click here to access/download;Figure;Figure 4.pdf](#)



a



b

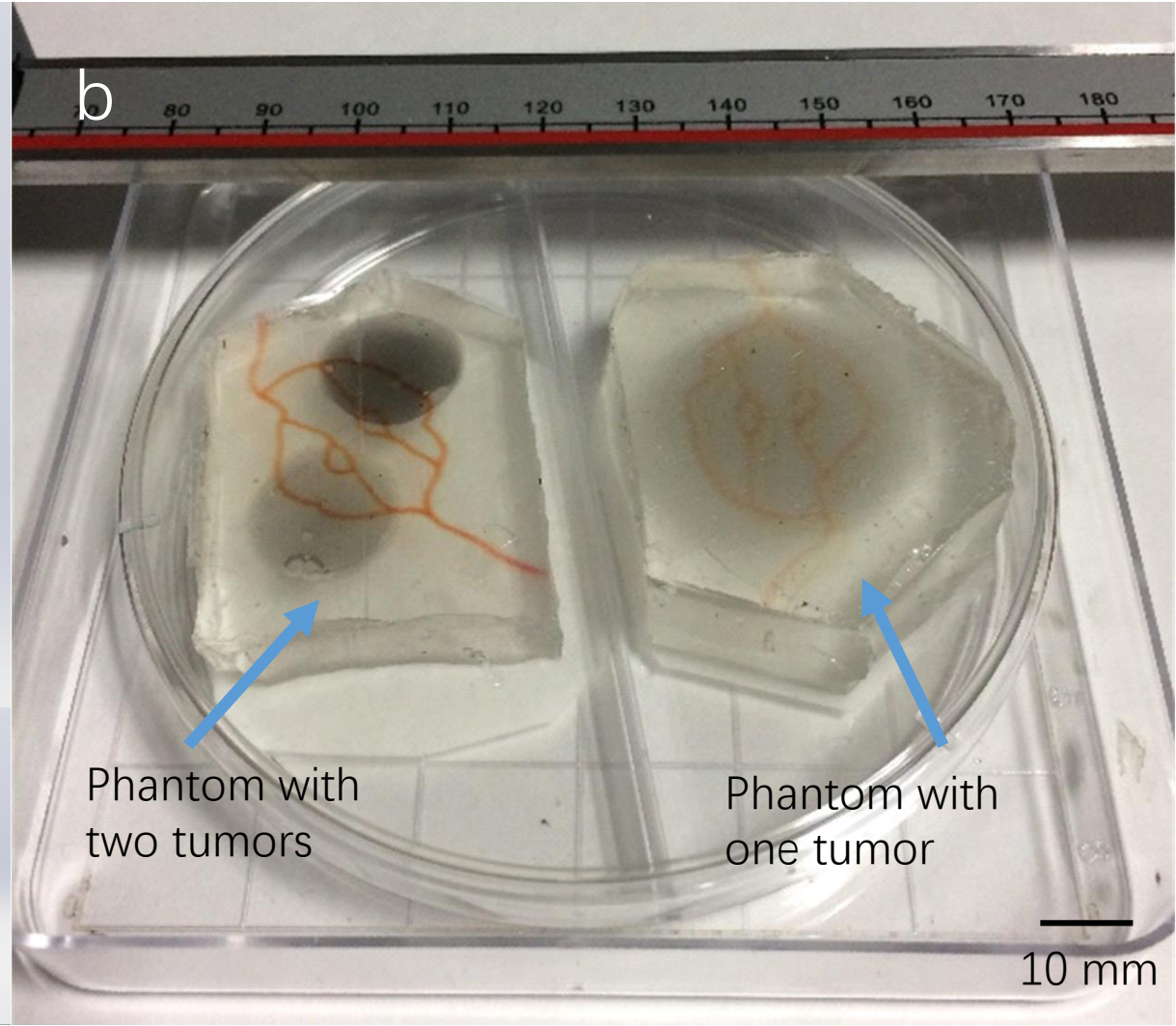
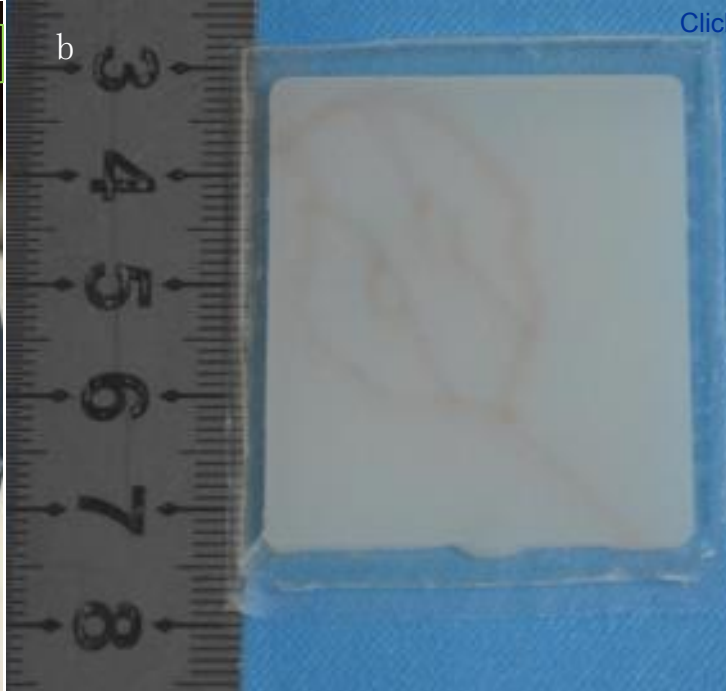
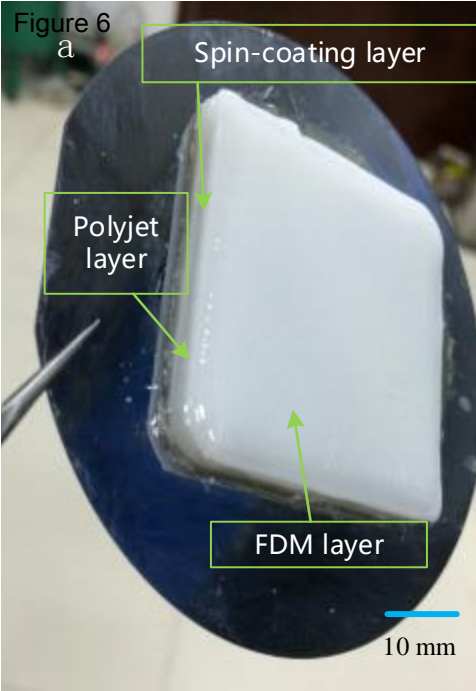
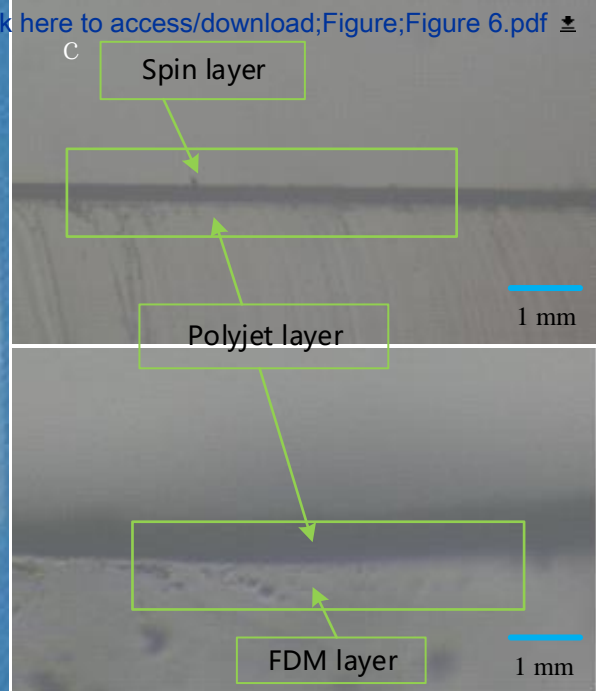




Figure 6



[Click here to access/download;Figure;Figure 6.pdf](#)



Name of Material/ Equipment	Company	Catalog Number	Comments/Description
2-Hydroxy-2-methylpropiophenone	aladdin	H110280-500g	Light initiator <a href="http://www.aladdin-e.com/custom-made">http://www.aladdin-e.com/custom-made</a> github: <a href="https://github.com/macanzhen/3D_printing_control_system_of_USTC">https://github.com/macanzhen/3D_printing_control_system_of_USTC</a>
3D printing control system	USTC	3DPrinter_control1.0	em_of_USTC
3D printing system	USTC	USTC-3DPrinter1.0	custom-made
AcroRip color	Human Plus Shenzhen CBD Technology Co.,Ltd.	AcroRip v8.2.6	
All-in-one nozzle slicing script	Juents		github: <a href="https://github.com/macanzhen/3D_printing_Cura_3.5.0">https://github.com/macanzhen/3D_printing_Cura_3.5.0</a>
Chinese Red Dye	Ultimaker	Cura_15.04.6	Oil-soluble
Cura	Shanghai Lida Industry Co.,Ltd.	LP	
Gel Wax			melting point: 56 °C Change object optical absorption parameters.
Graphite	aladdin	G103922-100g	<a href="http://www.aladdin-e.com/">http://www.aladdin-e.com/</a>
PDMS	Dow Corning		184
Titanium dioxide	ALDRICH	24858-100G	347 nm Photocured monomer
Triethylene glycol dimethacrylate	aladdin	T101642-250ml	<a href="http://www.aladdin-e.com/">http://www.aladdin-e.com/</a>
UV ink SLA Photopolymer Resin	time80s	RESIN-A	<a href="http://www.time80s.com/zlxz">http://www.time80s.com/zlxz</a>

all-in-one-nozzle-slicing-script

Dear reviewers:

Thank you for your time and effort to review our manuscript and video. We deeply appreciate your pertinent comment that helps us to improve our work. Based on your feedback, we have revised our video and manuscript. The following are our point-to-point responses, with your comment highlighted in italic font.

Editorial comments:

1. Please include the article ID number (60563) in the video file name in future submissions.

Sorry for missing the ID number in the file name of the previously submitted video, and we have added the number to the file name.

2. 2:45-2:47 - The audio quality of the narration addition here is too different from the rest of the narration. It sounds heavily filtered and artificial. This should be rerecorded with the same settings as the original narration.

The audio of this place was recorded using different types of equipment, therefore result in the difference in sounds. We re-recorded the explanation in this part and tried to make them similar to the rest of the narration.

3. 0:29, 1:17, and elsewhere: Please use 'mL' instead of 'ml'. Also, please ensure there is a space between numbers and their corresponding units (see 0:59).

We apologize for the mistakes in the video and have modified them in the revised video.

4. 2:10- 'AcroRIP' is commercial language; please use a generic term instead.

We deleted this part of the narration in the revised version of the video.

5. Results, 3: How exactly does Figure 4 demonstrate '[simulation of] different absorption and scattering parameters...'? Please clarify.

We apologize for the misunderstanding caused by the unclear explanation. In fact, the absorption and scattering parameters of a phantom depends on the ratio of the titanium dioxide and graphite powder inside. Figure 4 presents the phantoms of different feature sizes, printed by the FDM printing using the gel wax mixed titanium dioxide and graphite powder. We can change the ratio of supplying titanium dioxide and graphite powder during printing, and then phantoms (Figure 4b) of different absorption and scattering parameters are fabricated. The correlation of absorption and scattering parameters with the ratio of titanium dioxide and graphite powder can be found in the references [1].

## Reference

1, Liu, G. *et al.* Fabrication of a multilayer tissue-mimicking phantom with tunable optical properties to simulate vascular oxygenation and perfusion for optical imaging technology. *Applied optics*. **57** (23), 6772-6780 (2018).

6. Figure 2: What are the fit lines here (exponential decay?), and how well do they fit the data? Also, please use '60 s', not '60s' (include a space).

The fitting formula is  $y=a*(x^b)$ , and the fitting parameters and fitting degree results are as follows:

	a	b	R <sup>2</sup>
60 s	9439.5	0.824	0.9938
120 S	42488	0.979	0.9892
300 s	18954	0.81	0.9666

A space between the number and the unit in the picture has been added.

7. Figure 5a: What is the 'placing part', exactly?

We apologize for the misunderstanding caused by the description. The 'placing part' refers to the phantom simulating the subcutaneous tissue, which is cast by the polydimethylsiloxane (PDMS). To avoid the misleading, we have replaced them as 'casting part' in the revised manuscript and video.



8. Figure 5b: 'two tumors', not 'two tumor'.

We apologize for the misunderstanding caused by the mistake, and it has been corrected in the revised manuscript and video.

## ARTICLE AND VIDEO LICENSE AGREEMENT

Title of Article:	Multimodal Three-dimensional Printing of Phantoms to Simulate Biologic Tissue
Author(s):	Canzhen Ma, Shuwei Shen, Guangli Liu, Siyue Guo, Buyun Guo, Jialuo Li, Kuiming Huang, Yidan Zheng, Pengfei Shao, Erbao Dong, Ronald X. Xu

Item 1: The Author elects to have the Materials be made available (as described at <http://www.jove.com/publish>) via:



Standard Access



Open Access

Item 2: Please select one of the following items:



The Author is **NOT** a United States government employee.



The Author is a United States government employee and the Materials were prepared in the course of his or her duties as a United States government employee.



The Author is a United States government employee but the Materials were NOT prepared in the course of his or her duties as a United States government employee.

### ARTICLE AND VIDEO LICENSE AGREEMENT

1. **Defined Terms.** As used in this Article and Video License Agreement, the following terms shall have the following meanings: “**Agreement**” means this Article and Video License Agreement; “**Article**” means the article specified on the last page of this Agreement, including any associated materials such as texts, figures, tables, artwork, abstracts, or summaries contained therein; “**Author**” means the author who is a signatory to this Agreement; “**Collective Work**” means a work, such as a periodical issue, anthology or encyclopedia, in which the Materials in their entirety in unmodified form, along with a number of other contributions, constituting separate and independent works in themselves, are assembled into a collective whole; “**CRC License**” means the Creative Commons Attribution-Non Commercial-No Derivs 3.0 Unported Agreement, the terms and conditions of which can be found at: <http://creativecommons.org/licenses/by-nc-nd/3.0/legalcode>; “**Derivative Work**” means a work based upon the Materials or upon the Materials and other pre-existing works, such as a translation, musical arrangement, dramatization, fictionalization, motion picture version, sound recording, art reproduction, abridgment, condensation, or any other form in which the Materials may be recast, transformed, or adapted; “**Institution**” means the institution, listed on the last page of this Agreement, by which the Author was employed at the time of the creation of the Materials; “**JoVE**” means MyJoVE Corporation, a Massachusetts corporation and the publisher of The Journal of Visualized Experiments; “**Materials**” means the Article and / or the Video; “**Parties**” means the Author and JoVE; “**Video**” means any video(s) made by the Author, alone or in conjunction with any other parties, or by JoVE or its affiliates or agents, individually or in collaboration with the Author or any other parties, incorporating all or any portion

of the Article, and in which the Author may or may not appear.

2. **Background.** The Author, who is the author of the Article, in order to ensure the dissemination and protection of the Article, desires to have the JoVE publish the Article and create and transmit videos based on the Article. In furtherance of such goals, the Parties desire to memorialize in this Agreement the respective rights of each Party in and to the Article and the Video.

3. **Grant of Rights in Article.** In consideration of JoVE agreeing to publish the Article, the Author hereby grants to JoVE, subject to **Sections 4** and **7** below, the exclusive, royalty-free, perpetual (for the full term of copyright in the Article, including any extensions thereto) license (a) to publish, reproduce, distribute, display and store the Article in all forms, formats and media whether now known or hereafter developed (including without limitation in print, digital and electronic form) throughout the world, (b) to translate the Article into other languages, create adaptations, summaries or extracts of the Article or other Derivative Works (including, without limitation, the Video) or Collective Works based on all or any portion of the Article and exercise all of the rights set forth in (a) above in such translations, adaptations, summaries, extracts, Derivative Works or Collective Works and (c) to license others to do any or all of the above. The foregoing rights may be exercised in all media and formats, whether now known or hereafter devised, and include the right to make such modifications as are technically necessary to exercise the rights in other media and formats. If the “Open Access” box has been checked in **Item 1** above, JoVE and the Author hereby grant to the public all such rights in the Article as provided in, but subject to all limitations and requirements set forth in, the CRC License.

612542.6 For questions, please contact us at [submissions@jove.com](mailto:submissions@jove.com) or +1.617.945.9051.

## ARTICLE AND VIDEO LICENSE AGREEMENT

4. **Retention of Rights in Article.** Notwithstanding the exclusive license granted to JoVE in **Section 3** above, the Author shall, with respect to the Article, retain the non-exclusive right to use all or part of the Article for the non-commercial purpose of giving lectures, presentations or teaching classes, and to post a copy of the Article on the Institution's website or the Author's personal website, in each case provided that a link to the Article on the JoVE website is provided and notice of JoVE's copyright in the Article is included. All non-copyright intellectual property rights in and to the Article, such as patent rights, shall remain with the Author.

5. **Grant of Rights in Video – Standard Access.** This **Section 5** applies if the "Standard Access" box has been checked in **Item 1** above or if no box has been checked in **Item 1** above. In consideration of JoVE agreeing to produce, display or otherwise assist with the Video, the Author hereby acknowledges and agrees that, Subject to **Section 7** below, JoVE is and shall be the sole and exclusive owner of all rights of any nature, including, without limitation, all copyrights, in and to the Video. To the extent that, by law, the Author is deemed, now or at any time in the future, to have any rights of any nature in or to the Video, the Author hereby disclaims all such rights and transfers all such rights to JoVE.

6. **Grant of Rights in Video – Open Access.** This **Section 6** applies only if the "Open Access" box has been checked in **Item 1** above. In consideration of JoVE agreeing to produce, display or otherwise assist with the Video, the Author hereby grants to JoVE, subject to **Section 7** below, the exclusive, royalty-free, perpetual (for the full term of copyright in the Article, including any extensions thereto) license (a) to publish, reproduce, distribute, display and store the Video in all forms, formats and media whether now known or hereafter developed (including without limitation in print, digital and electronic form) throughout the world, (b) to translate the Video into other languages, create adaptations, summaries or extracts of the Video or other Derivative Works or Collective Works based on all or any portion of the Video and exercise all of the rights set forth in (a) above in such translations, adaptations, summaries, extracts, Derivative Works or Collective Works and (c) to license others to do any or all of the above. The foregoing rights may be exercised in all media and formats, whether now known or hereafter devised, and include the right to make such modifications as are technically necessary to exercise the rights in other media and formats. For any Video to which this **Section 6** is applicable, JoVE and the Author hereby grant to the public all such rights in the Video as provided in, but subject to all limitations and requirements set forth in, the CRC License.

7. **Government Employees.** If the Author is a United States government employee and the Article was prepared in the course of his or her duties as a United States government employee, as indicated in **Item 2** above, and any of the licenses or grants granted by the Author hereunder exceed the scope of the 17 U.S.C. 403, then the rights granted hereunder shall be limited to the maximum

rights permitted under such statute. In such case, all provisions contained herein that are not in conflict with such statute shall remain in full force and effect, and all provisions contained herein that do so conflict shall be deemed to be amended so as to provide to JoVE the maximum rights permissible within such statute.

8. **Protection of the Work.** The Author(s) authorize JoVE to take steps in the Author(s) name and on their behalf if JoVE believes some third party could be infringing or might infringe the copyright of either the Author's Article and/or Video.

9. **Likeness, Privacy, Personality.** The Author hereby grants JoVE the right to use the Author's name, voice, likeness, picture, photograph, image, biography and performance in any way, commercial or otherwise, in connection with the Materials and the sale, promotion and distribution thereof. The Author hereby waives any and all rights he or she may have, relating to his or her appearance in the Video or otherwise relating to the Materials, under all applicable privacy, likeness, personality or similar laws.

10. **Author Warranties.** The Author represents and warrants that the Article is original, that it has not been published, that the copyright interest is owned by the Author (or, if more than one author is listed at the beginning of this Agreement, by such authors collectively) and has not been assigned, licensed, or otherwise transferred to any other party. The Author represents and warrants that the author(s) listed at the top of this Agreement are the only authors of the Materials. If more than one author is listed at the top of this Agreement and if any such author has not entered into a separate Article and Video License Agreement with JoVE relating to the Materials, the Author represents and warrants that the Author has been authorized by each of the other such authors to execute this Agreement on his or her behalf and to bind him or her with respect to the terms of this Agreement as if each of them had been a party hereto as an Author. The Author warrants that the use, reproduction, distribution, public or private performance or display, and/or modification of all or any portion of the Materials does not and will not violate, infringe and/or misappropriate the patent, trademark, intellectual property or other rights of any third party. The Author represents and warrants that it has and will continue to comply with all government, institutional and other regulations, including, without limitation all institutional, laboratory, hospital, ethical, human and animal treatment, privacy, and all other rules, regulations, laws, procedures or guidelines, applicable to the Materials, and that all research involving human and animal subjects has been approved by the Author's relevant institutional review board.

11. **JoVE Discretion.** If the Author requests the assistance of JoVE in producing the Video in the Author's facility, the Author shall ensure that the presence of JoVE employees, agents or independent contractors is in accordance with the relevant regulations of the Author's institution. If more than one author is listed at the beginning of this Agreement, JoVE may, in its sole

## ARTICLE AND VIDEO LICENSE AGREEMENT

discretion, elect not take any action with respect to the Article until such time as it has received complete, executed Article and Video License Agreements from each such author. JoVE reserves the right, in its absolute and sole discretion and without giving any reason therefore, to accept or decline any work submitted to JoVE. JoVE and its employees, agents and independent contractors shall have full, unfettered access to the facilities of the Author or of the Author's institution as necessary to make the Video, whether actually published or not. JoVE has sole discretion as to the method of making and publishing the Materials, including, without limitation, to all decisions regarding editing, lighting, filming, timing of publication, if any, length, quality, content and the like.

12. **Indemnification.** The Author agrees to indemnify JoVE and/or its successors and assigns from and against any and all claims, costs, and expenses, including attorney's fees, arising out of any breach of any warranty or other representations contained herein. The Author further agrees to indemnify and hold harmless JoVE from and against any and all claims, costs, and expenses, including attorney's fees, resulting from the breach by the Author of any representation or warranty contained herein or from allegations or instances of violation of intellectual property rights, damage to the Author's or the Author's institution's facilities, fraud, libel, defamation, research, equipment, experiments, property damage, personal injury, violations of institutional, laboratory, hospital, ethical, human and animal treatment, privacy or other rules, regulations, laws, procedures or guidelines, liabilities and other losses or damages related in any way to the submission of work to JoVE, making of videos by JoVE, or publication in JoVE or elsewhere by JoVE. The Author shall be responsible for, and shall hold JoVE harmless from, damages caused by lack of sterilization, lack of cleanliness or by contamination due to

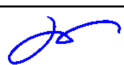
the making of a video by JoVE its employees, agents or independent contractors. All sterilization, cleanliness or decontamination procedures shall be solely the responsibility of the Author and shall be undertaken at the Author's expense. All indemnifications provided herein shall include JoVE's attorney's fees and costs related to said losses or damages. Such indemnification and holding harmless shall include such losses or damages incurred by, or in connection with, acts or omissions of JoVE, its employees, agents or independent contractors.

13. **Fees.** To cover the cost incurred for publication, JoVE must receive payment before production and publication of the Materials. Payment is due in 21 days of invoice. Should the Materials not be published due to an editorial or production decision, these funds will be returned to the Author. Withdrawal by the Author of any submitted Materials after final peer review approval will result in a US\$1,200 fee to cover pre-production expenses incurred by JoVE. If payment is not received by the completion of filming, production and publication of the Materials will be suspended until payment is received.

14. **Transfer, Governing Law.** This Agreement may be assigned by JoVE and shall inure to the benefits of any of JoVE's successors and assignees. This Agreement shall be governed and construed by the internal laws of the Commonwealth of Massachusetts without giving effect to any conflict of law provision thereunder. This Agreement may be executed in counterparts, each of which shall be deemed an original, but all of which together shall be deemed to be one and the same agreement. A signed copy of this Agreement delivered by facsimile, e-mail or other means of electronic transmission shall be deemed to have the same legal effect as delivery of an original signed copy of this Agreement.

A signed copy of this document must be sent with all new submissions. Only one Agreement is required per submission.

### CORRESPONDING AUTHOR

Name:	Ronald X. Xu	
Department:	Department of Precision Machinery and Precision Instrumentation	
Institution:	University of Science and Technology of China	
Title:	Multimodal Three-dimensional Printing of Phantoms to Simulate Biologic ...	
Signature:		Date: 09/19/2019

Please submit a **signed** and **dated** copy of this license by one of the following three methods:

1. Upload an electronic version on the JoVE submission site
2. Fax the document to +1.866.381.2236
3. Mail the document to JoVE / Attn: JoVE Editorial / 1 Alewife Center #200 / Cambridge, MA 02140

612542.6 For questions, please contact us at [submissions@jove.com](mailto:submissions@jove.com) or +1.617.945.9051.



# Signature Certificate

Document Ref.: B6NZT-C7X4F-RW6U8-RFZJS

Document signed by:

	<p><b>Canzhen Ma</b> Verified E-mail: mcanzhen@mail.ustc.edu.cn</p> <p>IP: 18.179.118.14      Date: 19 Sep 2019 08:13:27 UTC</p>	 
---	--	--

Document completed by all parties on:  
19 Sep 2019 08:13:27 UTC

Page 1 of 1



Signed with PandaDoc.com

PandaDoc is the document platform that boosts your company's revenue by accelerating the way it transacts.

